ECONSTOR
Make Your Publications Visible.

A Service of

ZBW Leibniz-Informationszentrum Wirtschaft
Leibniz Information Centre for Economics

Li, Su-Yuan et al.

Article — Published Version

Projected drought conditions in Northwest China with CMIP6 models under combined SSPs and RCPs for 2015–2099

Advances in Climate Change Research

Provided in Cooperation with:
Leibniz Institute of Agricultural Development in Transition Economies (IAMO), Halle (Saale)

Suggested Citation: Li, Su-Yuan et al. (2020) : Projected drought conditions in Northwest China with CMIP6 models under combined SSPs and RCPs for 2015–2099, Advances in Climate Change Research, ISSN 1674-9278, Elsevier, Amsterdam, Vol. 11, Iss. 3, pp. 210-217, https://doi.org/10.1016/j.accre.2020.09.003

This Version is available at:
https://hdl.handle.net/10419/230517

Standard-Nutzungsbedingungen:

Die Dokumente auf EconStor dürfen zu eigenen wissenschaftlichen Zwecken und zum Privatgebrauch gespeichert und kopiert werden.

Sie dürfen die Dokumente nicht für öffentliche oder kommerzielle Zwecke vervielfältigen, öffentlich ausstellen, öffentlich zugänglich machen, vertreiben oder anderweitig nutzen.

Sofern die Verfasser die Dokumente unter Open-Content-Lizenzen (insbesondere CC-Lizenzen) zur Verfügung gestellt haben sollten, gelten abweichend von diesen Nutzungsbedingungen die in der dort genannten Lizenz gewährten Nutzungsrechte.

Terms of use:

Documents in EconStor may be saved and copied for your personal and scholarly purposes.

You are not to copy documents for public or commercial purposes, to exhibit the documents publicly, to make them publicly available on the internet, or to distribute or otherwise use the documents in public.

If the documents have been made available under an Open Content Licence (especially Creative Commons Licences), you may exercise further usage rights as specified in the indicated licence.

https://creativecommons.org/licenses/by-nc-nd/4.0/

WWW.ECONSTOR.EU

Mitglied der Leibniz-Gemeinschaft

KeAi
CHINESE ROOTS
GLOBAL IMPACT

Available online at www.sciencedirect.com

ScienceDirect

Advances in Climate Change Research 11 (2020) 210–217

www.keaipublishing.com/en/journals/accr/

Projected drought conditions in Northwest China with CMIP6 models under combined SSPs and RCPs for 2015–2099

LI Su-Yuan[a], MIAO Li-Juan[b,c,*], JIANG Zhi-Hong[a], WANG Guo-Jie[b], GNYAWALI Kaushal Raj[d], ZHANG Jing[b], ZHANG Hui[b], FANG Ke[e], HE Yu[b], LI Chun[b]

[a] *School of Atmospheric Sciences, Nanjing University of Information Science & Technology, Nanjing, 210044, China*
[b] *School of Geographical Sciences, Nanjing University of Information Science & Technology, Nanjing, 210044, China*
[c] *Leibniz Institute of Agricultural Development in Transition Economies, Halle (Saale), 06120, Germany*
[d] *Natural Hazards Section, Himalayan Risk Research Institute, Bhaktapur, 44800, Nepal*
[e] *Shangyu Meteorological Bureau, Shaoxing, 312000, China*

Received 15 March 2020; revised 14 May 2020; accepted 3 September 2020
Available online 16 September 2020

Abstract

Northwest China is one of the most arid regions in the world and has experienced intriguing climate warming and humidification. Nonetheless, future climate conditions in Northwest China still remain uncertain. In this study, we applied an ensemble of the 12 latest model simulations of the Coupled Model Intercomparison Project Phase 6 (CMIP6) to assess future drought conditions until 2099 in Northwest China, as inferred from the Palmer Drought Severity Index (PDSI). Future drought conditions were projected under three climate change scenarios through the combination of shared socioeconomic pathways (SSPs) and representative concentration pathways (RCPs), namely, SSP126 (SSP1 + RCP2.6, a green development pathway), SSP245 (SSP2 + RCP4.5, an intermediate development pathway), and SSP585 (SSP5 + RCP8.5, a high development pathway). For 2015–2099, drought severity showed no trend under SSP126, in contrast, for the SSP245 and SSP585 scenarios, a rapid increase during 2015–2099 was observed, especially under SSP585. We also found that the drought frequency in Northwest China under SSP585 was generally lower than that under SSP126 and SSP245, although the drought duration under SSP585 tended to be longer. These findings suggest the green development pathway in drought mitigation and adaptation strategies in Northwest China, an arid and agricultural region along the Silk Road.

Keywords: Climate change; Drought; CMIP6; PDSI; Dryland; Northwest China

1. Introduction

Climate change and climate extremes have become global concerns in recent years (Degefu and Bewket, 2014; Gaffin et al., 2004). The IPCC Fifth Assessment Report (AR5) (IPCC, 2018) noted that a 0.85 °C increase in the global annual mean temperature has occurred in 1880–2012 and that global warming has directly increased meteorological disasters, e.g., droughts, floods and typhoons (Capra et al., 2013). Drylands are some of the most vulnerable regions affected by ongoing climate warming and droughts (Dai, 2013; Huang et al., 2017). Droughts tend to occur in drylands due to insufficient rainfall and few rainfall events (Dai, 2011). Droughts can lead to water scarcity, crop failure, land degradation and soil erosion, which have important effects on the sustainable development of local agriculture and the economy (He et al., 2014; Sternberg, 2018).

* Corresponding author. School of Geographical Sciences, Nanjing University of Information Science & Technology, Nanjing, 210044, China.
E-mail address: miaolijuan1111@gmail.com (MIAO L.-J.).
Peer review under responsibility of National Climate Center (China Meteorological Administration).

https://doi.org/10.1016/j.accre.2020.09.003
1674-9278/Copyright © 2020, National Climate Center (China Meteorological Administration). Production and hosting by Elsevier B.V. on behalf of KeAi. This is an open access article under the CC BY-NC-ND license (http://creativecommons.org/licenses/by-nc-nd/4.0/).

Northwest China is regarded as one of the driest regions in the world; the fragile eco-environment in this area is vulnerable to climate change and climate extremes. Northwest China is also located in a region of complex topography, e.g., from high mountains (Tianshan, Kunlun and Qilian) to desert basins (Tarim, Junggar and Qaidam) (Liu et al., 2016), and geographically includes five provinces (e.g., Xinjiang, Qinghai, Gansu, Shaanxi and Ningxia). In recent decades, droughts have been regarded as one of the most concerning meteorological disasters in Northwest China (Sternberg, 2018). In general, from the 1960s to the 2010s, climate conditions in Northwest China tended to be warmer and more humid, i.e., a relief in drought occurrence (Wang and Qin, 2017; Yang et al., 2018b; Yuan et al., 2017; Shi et al., 2002). For the future, Northwest China is projected to become drier in 2016−2050 based on CMIP5 model simulations (Huang et al., 2018). Conversely, Wang and Chen (2014) found that there is no obvious dryness tendency over Northwest China for the beginning of the century (2010−2039) and mid-century (2040−2099), which is in line with the increasing trend of precipitation. Concerning these controversies underlying the projected changes in drought conditions over Northwest China, reliable evidence to quantify such changes is certainly needed.

There are large varieties of indices aimed at quantitatively detecting droughts at global and regional scales (Dai, 2011; Liu et al., 2016), e.g., the Palmer Drought Severity Index (PDSI), the Standardized Precipitation Index (SPI) and the Standardized Precipitation Evapotranspiration Index (SPEI) (Palmer, 1965; Svoboda et al., 2012; Vicente-Serrano et al., 2010). The PDSI accounts for the effect of evaporation computed by primary (precipitation) and secondary (surface air temperature) variables for capturing meteorological droughts, according to the principle of the soil water balance (Dai, 2011). The PDSI is a standardized indicator with a close relation to moisture availability, which can be expressed as the water content of the upper 1-m soil layer (Mika et al., 2005). The SPI is determined solely by precipitation, and the SPEI is calculated based on the difference between precipitation and potential evapotranspiration (PET), regardless of the soil water balance. The PDSI, however, has been shown to be closely related to the true soil water balance based on a supply and demand model of soil moisture (Palmer, 1965; Su et al., 2018). The advantage of the PDSI has also been supported by recent studies in Northwest China and adjacent regions. For example, Huang et al. (2018) found that drought events determined by the SPEI alone might overestimate the number of actual drought events during 1961−2005 in Northwest China, and, based on the PDSI, the estimated drought occurrence was captured more than 90% of the time during 2001−2010 in China (Liang et al., 2017).

The occurrence of droughts generally results from many factors, such as meteorological anomalies, solar activity, land surface physical processes, and human activities (van Loon et al., 2016; Zhang et al., 2017). In Northwest China, the impact of human activities (e.g., socioeconomic factors) should never be ignored (Wang et al., 2004; Zhou et al., 2015). For example, a recent study reported that human activities accounted for the 70.3% of the expansion of desertification in Northwest China, while the contribution of climate change is lower, only 21.7% (Zhou et al., 2015). Therefore, model simulations from Coupled Model Intercomparison Project Phase 6 (CMIP6), considering both socioeconomic and climate change factors, could be regarded as a reasonable source for future climate predictions in Northwest China. Here, we aimed to gain the two following achievements: 1) has Northwest China experienced a warm-wet climate over the past century, and 2) will the drought conditions of Northwest China continue to be relieved or become worse during the next 100 years? Considering both socioeconomic and climatic factors, this study could facilitate the formation of mitigation and adaptation strategies for drought-related economic loss in Northwest China.

2. Data and methods

2.1. Study area

Northwest China (87°−120°E, 41°−53°N) occupies ~33% of the total land area of China (Fig. 1). Its land cover is dominated by grasslands and barren areas, and it features limited precipitation and frequent droughts (Miao et al., 2015). Annual precipitation varies from ~200 mm to 1250 mm, which is mostly concentrated in the rainy season from June to September (Liu et al., 2016).

2.2. Datasets

2.2.1. Observations

Monthly temperature and precipitation data spanning 1961−2016 from 201 meteorological stations (Fig. 1) were provided by the National Meteorological Information Center, China Meteorological Administration. We interpolated the station-based datasets to a spatial resolution of 0.5° × 0.5° by applying the Cressman interpolation method (Cressman, 1959).

2.2.2. Model simulations

Historical and future climate simulations from 1850 to 2100 were extracted from CMIP6 model outputs (https://esgf-node.llnl.gov/projects/cmip6/). The 12 models listed in Table 1 were used. The models consider both shared socioeconomic pathways (SSPs) and representative concentration pathways (RCPs). The simulations from three scenarios were selected, i.e., SSP126, SSP245 and SSP585. SSP126 is the updated scenario of RCP2.6 that uses a sustainable world that takes a green pathway, with (SSP1)-RCP2.6 forcing at a low level of greenhouse gas emissions; SSP245 is the updated scenario of RCP4.5 that uses a moderate world, with (SSP2)-RCP4.5 forcing at an intermediate level of greenhouse gas emissions; and SSP585 is the updated scenario of RCP8.5 that uses a world with rapid fossil fuel evolution, with (SSP5)-RCP8.5 (O'Neill et al., 2014, 2017) forcing at a high level of greenhouse gas emissions (Gillett et al., 2016; Zhang et al., 2019a).

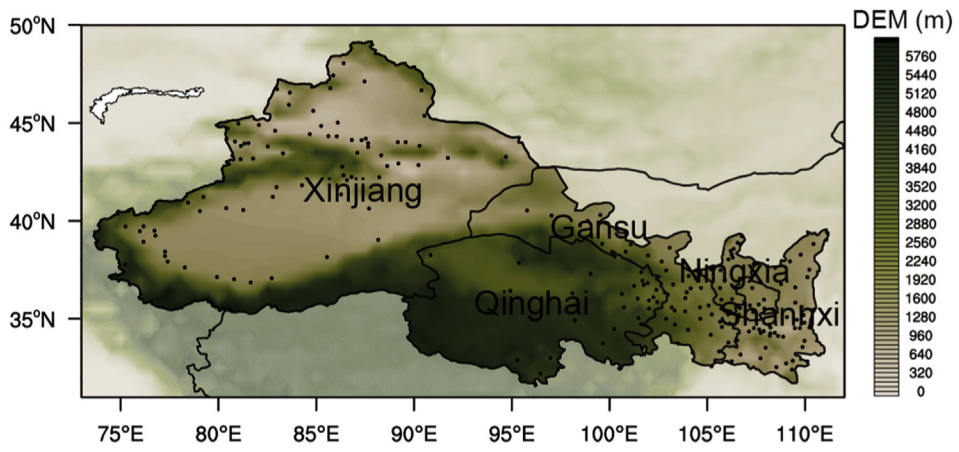

Fig. 1. Geographical map of Northwest China (The black dots indicate the locations of the meteorological stations).

2.3. Methods

2.3.1. Data preprocessing

Preprocessing of the CMIP6 data included bias correction based on the observation data (1961–2014) by the equidistant cumulative distribution function (EDCDF) method (Li et al., 2010). We applied the EDCDF method to adjust the cumulative distribution function (CDF) of CMIP6 model simulations according to their differences from observation-based CDFs (Li et al., 2010). Compared with the traditional quantile-based matching method (e.g., the CDF method), the EDCDF method is relatively efficient at reducing biases across China (Yang et al., 2018a). Subsequently, the ensemble mean results were acquired by averaging the 12 models covering the period of 1850–2099. Note that data in 2100 were excluded due to the lack of specific model outputs. We divided the entire study period into the historical period (1850–2014) and the future period (2015–2099).

2.3.2. PDSI

The PDSI was originally developed by Palmer in 1965 and accounts for both precipitation (as the primary variable) and surface air temperature (as the secondary variable) (Palmer, 1965) (see Appendix for more details). We categorized the drought severity (i.e., PDSI values) into four groups, including near-normal dry (−1.99 to 0), moderately dry (approximately −2.99 to −2.0), severely dry (approximately −3.99 to −3.0), and extremely dry conditions (≤−4.0) (Palmer, 1965). The arid areas are defined as regions that are moderately, severely and extremely dry according to the original PDSI values. Here, for each drought event, the beginnings and ends are based on the drought conditions, i.e., PDSI ≤ -2.0. The drought severity, drought frequency, and duration of drought events are computed at the pixel level. The drought-affected area is extracted from the sum of regions where the PDSI is below −2.0. Meanwhile, the duration of drought event is defined as the time interval during which the PDSI is lower than −2.0. The frequency of drought events (N') is expressed in terms of the number of drought events per 100 years (McCabe et al., 2004) as follows:

$$N' = \frac{N}{t} \times 100 \tag{1}$$

where N is the frequency of the drought events in the historical period (1850–2014, $t = 165$) or in 2015–2099 ($t = 85$).

Table 1
Detailed information on the 12 CMIP6 climate models.

Model	Source	Spatial resolution (lat × lon)
BCC-CSM2-MR	Beijing Climate Center, China	1.125° × 1.125°
CAMS-CSM1-0	Chinese Academy of Meteorological Sciences, China	1.125° × 1.125°
CanESM5	Canadian Centre for Climate Modelling and Analysis, Canada	2.8125° × 2.8125°
CESM2-WACCN	Climate and Global Dynamics Laboratory, USA	0.9375° × 1.25°
FGOALS-g3	The State Key Laboratory of Numerical Modeling for Atmospheric Sciences and Geophysical Fluid Dynamics (LASG), China	2.25° × 2°
GFDL-ESM4	Geophysical Fluid Dynamics Laboratory, USA	1° × 1.25°
ISPL-CM6A-LR	Institute Pierre-Simon Laplace, France	1.26° × 2.5°
MIROC6	Atmosphere and Ocean Research Institute, Japan	1.40625° × 1.40625°
MIROC-ES2L	Japan Agency for Marine-Earth Science and Technology, Japan	2.8125° × 2.8125°
MRI-ESM2-0	Meteorological Research Institute, Japan	1.125° × 1.125°
NESM3	Nanjing University of Information Science and Technology, China	1.875° × 1.875°
UKESM1	Met Office Hadley Centre, UK	1.25° × 1.875°

3. Results

3.1. Bias correction of CMIP6 model simulations

The EDCDF method was used to correct the time series of the temperature/precipitation observations extracted from the CMIP6 model simulations (see Methods). Compared with the simulations before bias correction, we found that the CMIP6 model simulations corrected by the EDCDF method are generally closer to the observations (station-based datasets) (1961–2014) and capable of reproducing the temporal trends in observed climatic variables.

3.2. Historical and future climate changes

Based on the ensemble mean of 12 CMIP6 model simulations, we present the historical and future annual mean temperature and total precipitations in Fig. 2. The overall tendency of the model simulation and observation is consistent (Fig. 2a and b). In the historical period (1850–2014), the annual mean temperature increased considerably by 0.84 °C from 3.59 °C (1850) to 4.43 °C (2014), with a warming rate of 0.05 °C per decade (Fig. 2a). Meanwhile, the historical annual total precipitation increased slightly from 208 mm to 225 mm (Fig. 2b). In the future period (2015–2099), the annual mean temperature is projected to increase at rates of 0.06 °C, 0.26 °C and 0.59 °C per decade under SSP126, SSP245 and SSP585, respectively (Fig. 2c). The warming rates under SSP245 and SSP585 were much higher than those in the historical period and under SSP126. The annual total precipitation is projected to increase slightly at rates of 5.6 mm, 6.4 mm and 8.0 mm per decade under the three scenarios (Fig. 2d). Overall, steep increase tendencies in both the temperature and precipitation are projected in the future, especially under SSP585.

3.3. Historical and future drought conditions

The drought severity increased separately from 1850 to the late 1870s and from the 1890s to the 1920s and then recovered from the 1940s to the mid-1980s, increasing again since the mid-1980s (Fig. 3a). Moreover, we found good agreement in drought severity and the percentage of arid area. Small arid area occurred from the 1940s to the mid-1980s (Fig. 3b), with the arid area percentage reaching a maximum of 54% in 1877 and a relatively low value of 4% in 1985. In summary, Northwest China experienced humidification from the 1940s to the mid-1980s.

In the future period (2015–2099), under SSP245 and SSP585, the drought severity is projected to increase, especially under SSP585, while the PDSI under SSP126 is projected to oscillate around zero (Fig. 3c). Correspondingly, the proportions of arid areas are projected to continue to increase at rates of 2.0% and 7.6% per decade under SSP245 and SSP585, respectively (Fig. 3d). In general, an increasing dryness trend is projected in the future period under SSP245 and SSP585, while no trend is observed under SSP126.

In the historical period, an increasing wetness trend dominated the western and central regions of Northwest China, while an increasing dryness trend was detected in the eastern region (Fig. 4e). In the future period, the spatial distribution of trends in drought severity differed across the three

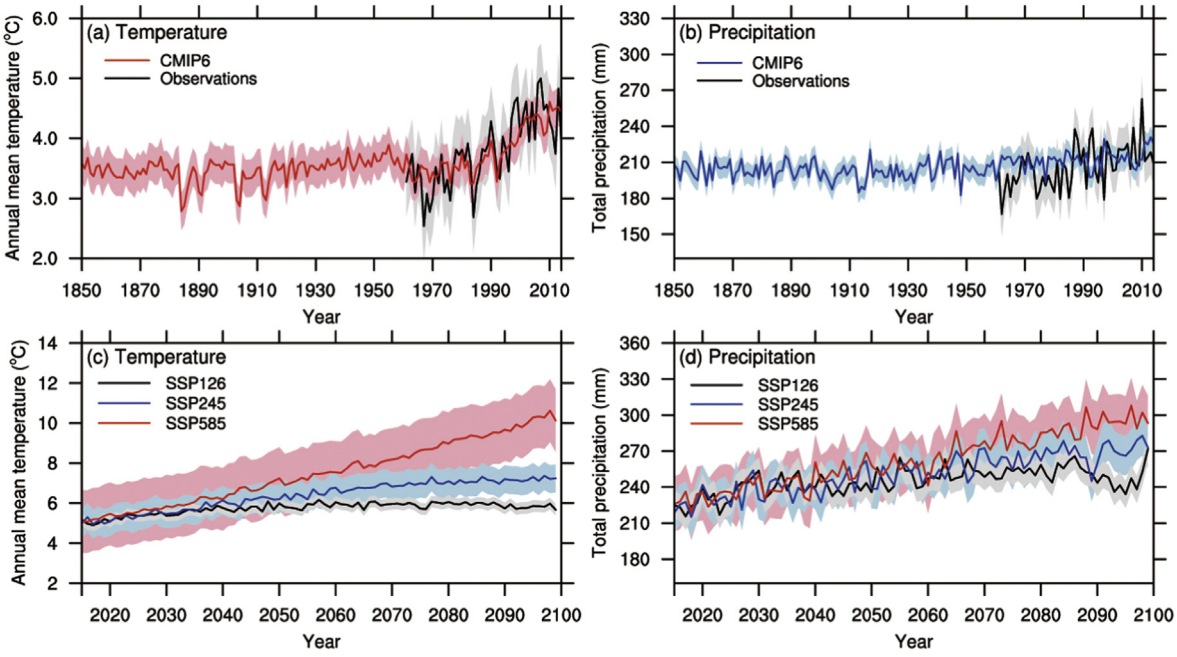

Fig. 2. Variations in annual mean temperature and total precipitation in Northwest China, (a) mean temperature, (b) total precipitation in 1850–2014 from the observations (station-based datasets) and CMIP6 model simulations, (c) mean temperature and (d) total precipitation in 2015–2099 under SSP126, SSP245 and SSP585 (The shaded area indicates the average value and corresponding standard deviation).

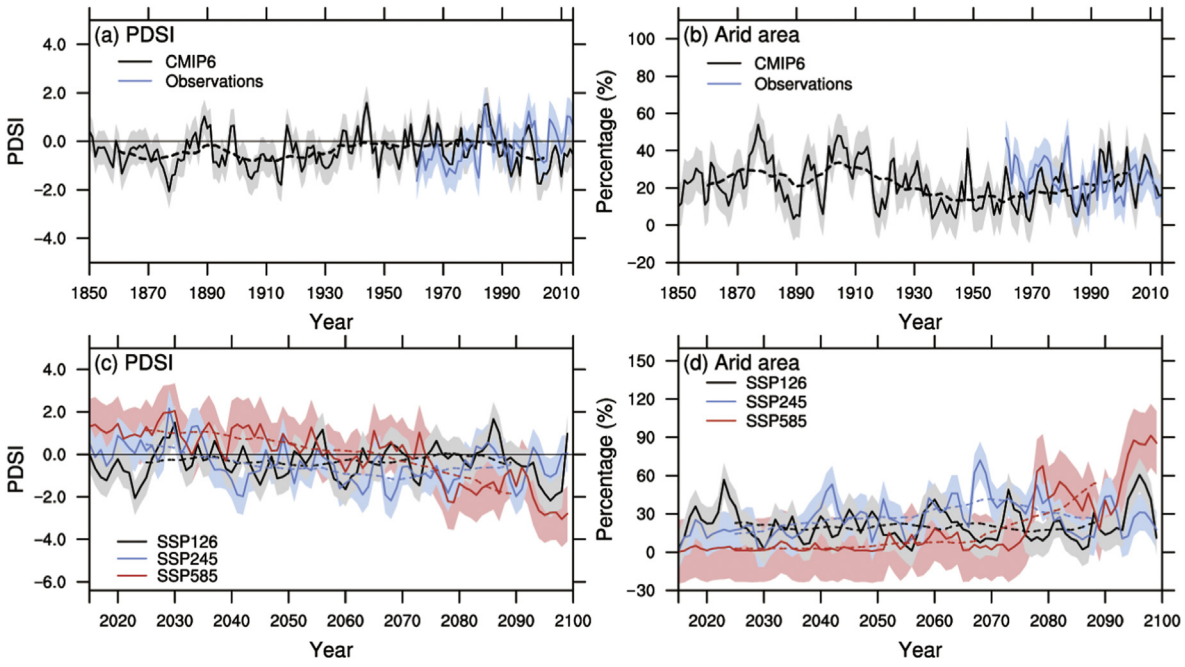

Fig. 3. Variations in the PDSI values (a, c) and the percentage of arid areas (b, d) for the periods in 1850–2014 (a, b) and 2015–2099 (c, d) (The shaded area indicates the standard deviation, and the dashed line presents the low-pass filtering results with a window of 21 years).

scenarios (Fig. 4f–h). A significant increasing dryness trend in the northern part of Northwest China and an increasing wetness trend in the southeastern region were identified under SSP126 (Fig. 4f). Under SSP245, the northern and eastern parts of Northwest China are projected to become even drier, while an increasing wetness tendency is expected in the southern region (Fig. 4g). Under SSP585, however, a significant tendency of dryness is observed across the entire region of Northwest China (Fig. 4h), which is more severe than the other two scenarios. In general, northern Xinjiang is projected to experience a larger increase in drought severity compared with the other provinces (Fig. 4f–h).

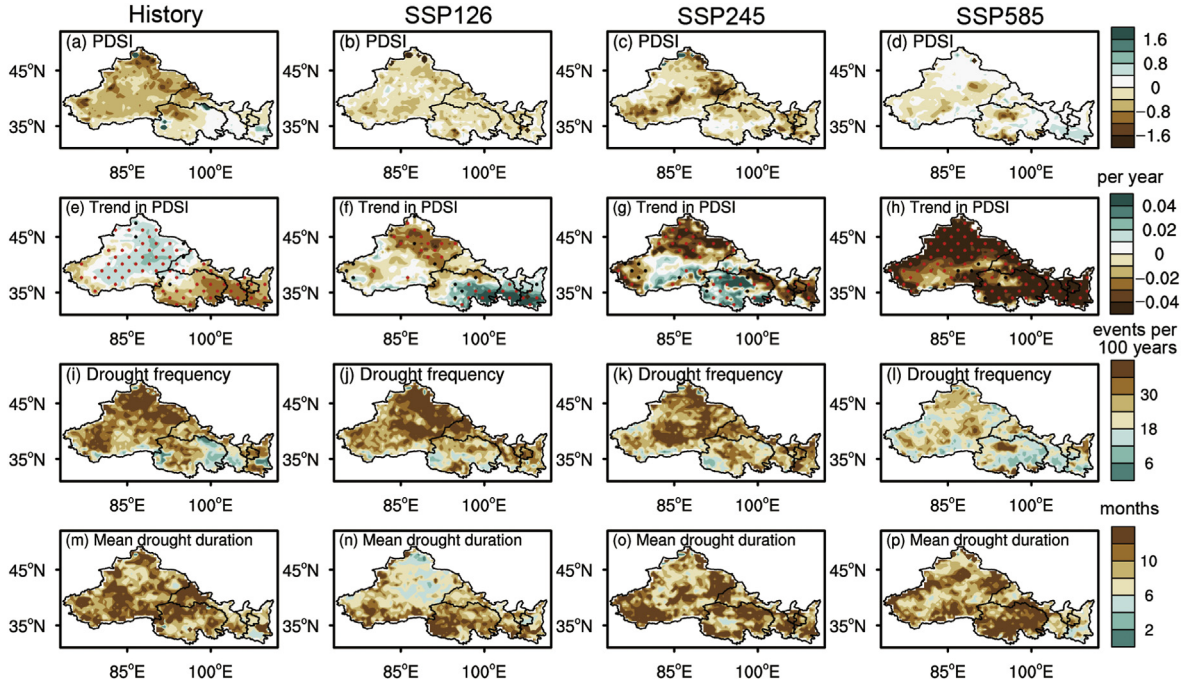

Fig. 4. Spatial patterns of the average (a–d) PDSI, (e–h) trends in PDSI (per year), (i–l) frequency of drought events (number of drought events per 100 years), and (m–p) mean duration of drought events based on the PDSI in the historical (1850–2014) and future (2015–2099) periods with CMIP6 models (The red and black dots in (e–h) illustrate the trends statistically significant at the 1% and 5% levels, respectively).

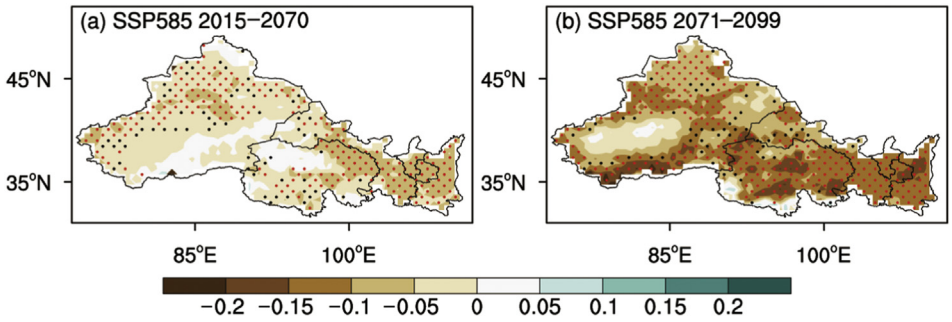

Fig. 5. Trends in the PDSI (per year) in (a) 2015–2070 and (b) 2071–2099 under SSP585 (The red and black dots illustrate the trends statistically significant at the 1% and 5% levels, respectively).

During 1850–2014, drought events more frequently occurred in the western region of Northwest China, with more than 30 continuous drought events per 100 years (Fig. 4i). The mean duration of these drought events was approximately 8–12 months (Fig. 4m). Qinghai, Gansu and Shaanxi were characterized by a lower drought frequency (6–18 times) and comparable drought duration (8–12 months) (Fig. 4i and m).

We observed projections with higher frequencies of drought events under SSP126 and SSP245 than under SSP585. Under SSP585, the drought frequency is projected to be lower but with longer duration than those under SSP126 and SSP245 (Fig. 4i–l). The mean drought duration under SSP126 is generally shorter than those under SSP245 and SSP585, especially in Xinjiang province (Fig. 4n–p).

As mentioned above, under SSP585, the entire region of Northwest China will be drier than the other two scenarios (Fig. 4h), which raises questions about whether there are differences in the drought severity between the early future period (2015–2070) and the later future period (2071–2099) (Fig. 5). In both periods, a significant dryness trend is observed across most of Northwest China. However, dryness is projected to be more severe in the later future period (2071–2099) under SSP585 than that in the early future period (2015–2070).

We also found dryness trends in Xinjiang under all three scenarios, and an increasing dryness trend under SSP245 and SSP585 is expected in Gansu, Ningxia and Shaanxi (Fig. 6a). Fig. 6a also demonstrates the order of the average changes in the PDSI values under the three scenarios in the future period, i.e., Xinjiang, Ningxia, Gansu, Shaanxi, and Qinghai. The order of the average percentage of arid area among the five provinces under the three scenarios is Ningxia (23.1%), Xinjiang (22.2%), Gansu (21.7%), Qinghai (21.4%), and Shaanxi (20.5%) (Fig. 6b). In terms of the drought trends and drought-affected areas, Xinjiang and Ningxia are projected to experience the most serious drought conditions for the period 2015–2099.

4. Discussion

In this study, we provided a comprehensive and timely analysis regarding past and future changes in Northwest China's drought conditions. Previous studies have formed the consensus that an overall warm-wet climate occurred over Northwest China, although their temporal and spatial coverage differed (Yang et al., 2018b; Chen and Sun, 2015). Our study enriched such finding over a longer historical period (1850–2014). We supported the projection that Northwest China will become drier (Yao et al., 2020). Interestingly, compared with the results under RCP4.5 and RCP8.5 based on CMIP5 (Huang et al., 2018; Mo et al., 2018), we found that drought occurrence under SSP585 is characterized with lower frequency but longer duration.

Changes in drought conditions over Northwest China could be mainly explained by the vital roles of precipitation and evapotranspiration (Zhang et al., 2019c). Enhanced evapotranspiration is associated with an increase in the surface vapor

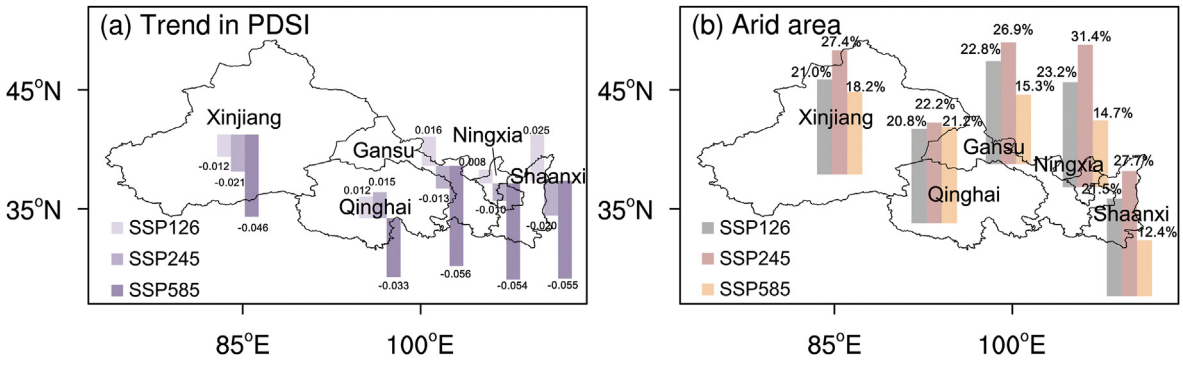

Fig. 6. Future drought projections at the provincial level under SSP126, SSP245 and SSP585 in 2015–2099, (a) linear trends in PDSI (per year) and (b) average percentage of arid area.

pressure deficit, which could cause widespread droughts (Dai and Zhao, 2017; Miao et al., 2020). When evapotranspiration exceeds precipitation, Northwest China will experience more severe drought conditions (Huang et al., 2018). In Northwest China, the increment in future evapotranspiration is expected to be 2−3 times larger than that in future precipitation, especially after approximately 2080 (Zhang et al., 2019b). Based on the CMIP6 models, the drought severity is projected to be more severe in the later future period (2071−2099) under SSP585. It is suggested that changes in evapotranspiration may be a determining factor for predicting the drought conditions in Northwest China in the late 21st century.

Compared with the previous studies, this study considered socioeconomic factors (e.g., SSP scenarios in CMIP6 models) in the projecting drought conditions in Northwest China, where the impact of human activities on drought occurrences cannot be ignored. Moreover, compared with CMIP5, CMIP6 models show improvements with the simulation of temperature and precipitation in Northwest China (Zhu et al., 2020), which are key factors to better capture the drought conditions. The CMIP6 data, therefore, could be used as a reasonable source to predict future climate characteristics in Northwest China. However, we found there is cold bias in most of the 12 CMIP6 models (except CESM2-WACCN, MIROC6, and MIROC-ES2L) and the ensemble means, and unanimous wet bias. This probably induced the underestimation of the future drought conditions in Northwest China. The inconsistency in the bias of temperature between the 12 CMIP6 models reminds that more models should be involved when temperature is considered in Northwest China. And CMIP6 GCMs might not reproduce the influence of a complex topography well in Northwest China (Cheng et al., 2015). Further model improvements in CMIP6 models could reduce model uncertainty but are still challenging.

5. Conclusion

Taking advantage of 12 CMIP6 model ensemble simulations and the PDSI, we presented the spatial−temporal patterns of drought conditions in Northwest China over historical and future periods. In line with previous studies, accompanied with significant increases in temperature and precipitation, alleviated drought conditions are prevalently observed in Northwest China from the 1940s to the mid-1980s. Such trends, however, are reversed in the next 100 years (i.e., 2015−2099). Our study suggested an increasing trend in dryness over Northwest China under intermediate to high greenhouse gas emission scenarios (e.g., SSP245, SSP585), especially under SSP585. Moreover, the occurrence of drought events in Northwest China is characterized as less frequent but longer duration under SSP585 than that under SSP126 and SSP245. Our study, therefore, provides a clear map showing the temporal evolution of drought conditions in Northwest China, which could be used as a basis to support climate adaptation strategies and policies to cope with future drought conditions and drought-related loss.

Declaration of competing interest

The authors declare no conflicts of interest.

Acknowledgments

This study was financially supported by the National Key Research and Development Program of China (2017YFA0603804), and the Key Project of National Social and Scientific Fund Program (16ZDA047), the European Union's Framework Programme for Research and Innovation Horizon 2020 (2014−2020) under the Marie Skłodowska-Curie Agreement (795179), and the Alexander von Humboldt Foundation of Germany, and Postgraduate Research & Practice Innovation Program of Jiangsu Province (SJKY19_0961). We specially thank Prof. Jiang Tong and his research team from the School of Geographical Sciences, Nanjing University of Information Science & Technology, for providing the bias-corrected CMIP6 datasets derived from the EDCDF method.

Appendix A. Supplementary data

Supplementary data to this article can be found online at https://doi.org/10.1016/j.accre.2020.09.003.

References

Capra, A., Consoli, S., Scicolone, B., 2013. Long-term climatic variability in Calabria and effects on drought and agrometeorological parameters. Water Resour. Manag. 27 (2), 601−617. https://doi.org/10.1007/s11269-012-0204-0.

Chen, H., Sun, J., 2015. Changes in drought characteristics over China using the standardized precipitation evapotranspiration index. J. Clim. 28 (13), 5430−5447. https://doi.org/10.1175/JCLI-D-14-00707.1.

Cheng, A., Feng, Q., Fu, G., et al., 2015. Recent changes in precipitation extremes in the Heihe River basin, Northwest China. Adv. Atmos. Sci. 32 (10), 1391−1406. https://doi.org/10.1007/s00376-015-4199-3.

Cressman, G.P., 1959. An operational objective analysis system. Mon. Wea. Rev. 87 (10), 367−374. https://doi.org/10.1175/1520-0493(1959)087<0367:AOOAS>2.0.CO;2.

Dai, A., 2011. Drought under global warming: a review. Wires Clim. Change 2 (1), 45−65. https://doi.org/10.1002/wcc.81.

Dai, A., 2013. Increasing drought under global warming in observations and models. Nat. Clim. Change. 3 (1), 52−58. https://doi.org/10.1038/NCLIMATE1633.

Dai, A., Zhao, T., 2017. Uncertainties in historical changes and future projections of drought. Part I: estimates of historical drought changes. Clim. Change. 144 (3), 519−533. https://doi.org/10.1007/s10584-016-1705-2.

Degefu, M.A., Bewket, W., 2014. Variability and trends in rainfall amount and extreme event indices in the Omo-Ghibe River Basin, Ethiopia. Reg. Environ. Change. 14 (2), 799−810. https://doi.org/10.1007/s10113-013-0538-z.

Gaffin, S.R., Rosenzweig, C., Xing, X., et al., 2004. Downscaling and geospatial gridding of socio-economic projections from the IPCC special Report on emissions scenarios (SRES). Glob. Environ. Change. 14 (2), 105−123. https://doi.org/10.1016/j.gloenvcha.2004.02.004.

Gillett, N., Shiogama, H., Funke, B., et al., 2016. The detection and attribution model Intercomparison Project (DAMIP v1. 0) contribution to CMIP6. Geosci. Model. Dev. 9, 3685−3697. https://doi.org/10.5194/gmd-9-3685-2016.

He, B., Cui, X., Wang, H., et al., 2014. Drought: the most important physical stress of terrestrial ecosystems. Acta. Ecol. Sin. 34 (4), 179−183. https://doi.org/10.1016/j.chnaes.2014.05.004.

Huang, J., Li, Y., Fu, C., et al., 2017. Dryland climate change: recent progress and challenges. Rev. Geophys. 55 (3), 719−778. https://doi.org/10.1002/2016RG000550.

Huang, J., Zhai, J., Jiang, T., et al., 2018. Analysis of future drought characteristics in China using the regional climate model CCLM. Clim. Dynam. 50 (1−2), 507−525. https://doi.org/10.1007/s00382-017-3623-z.

IPCC, 2018. An IPCC special report on the impacts of global warming of 1.5 °C above pre-industrial levels and related global greenhouse gas emission pathways, in the context of strengthening the global response to the threat of climate change, sustainable development, and efforts to eradicate poverty. http://www.ipcc.ch/report/sr15/.

Li, H., Sheffield, J., Wood, E.F., 2010. Bias correction of monthly precipitation and temperature fields from Intergovernmental Panel on Climate Change AR4 models using equidistant quantile matching. J. Geophys. Res. Atmos. 115, D10101. https://doi.org/10.1029/2009JD012882.

Liang, Y., Wang, Y., Yan, X., et al., 2018. Projection of drought hazards in China during twenty-first century. Theor. Appl. Climatol. 133, 331−341. https://doi.org/10.1007/s00704-017-2189-3.

Liu, Z., Menzel, L., Dong, C., et al., 2016. Temporal dynamics and spatial patterns of drought and the relation to ENSO: a case study in Northwest China. Int. J. Climatol. 36 (8), 2886−2898. https://doi.org/10.1002/joc.4526.

McCabe, G.J., Palecki, M.A., Betancourt, J.L., 2004. Pacific and Atlantic Ocean influences on multidecadal drought frequency in the United States. Proc. Natl. Acad. Sci. U. S. A. 101 (12), 4136−4141. https://doi.org/10.1073/pnas.0306738101.

Miao, L., Ye, P., He, B., et al., 2015. Future climate impact on the desertification in the dry land Asia using AVHRR GIMMS NDVI3g data. Remote. Sens. Basel. 7 (4), 3863−3877. https://doi.org/10.3390/rs70403863.

Miao, L., Li, S., Zhang, F., et al., 2020. Future drought in the dry lands of Asia under the 1.5 and 2.0 °C warming scenarios. Earth's Future. 8, e2019EF001337 https://doi.org/10.1029/2019EF001337.

Mika, J., Horvath, S., Makra, L., et al., 2005. The Palmer Drought Severity Index (PDSI) as an indicator of soil moisture. Phys. Chem. Earth. 30 (1−3), 223−230. https://doi.org/10.1016/j.pce.2004.08.036.

Mo, X., Hu, S., Lu, H., et al., 2018. Drought trends over the terrestrial China in the 21st century in climate change scenarios with ensemble GCM projections. J. Nat. Resour. 33 (7), 1244−1256. https://doi.org/10.1016/10.31497/zrzyxb.20170666 (in Chinese).

O'Neill, B.C., Kriegler, E., Riahi, K., et al., 2014. A new scenario framework for climate change research: the concept of shared socioeconomic pathways. Clim. Change. 122 (3), 387−400. https://doi.org/10.1007/s10584-013-0905-2.

O'Neill, B.C., Kriegler, E., Ebi, K.L., et al., 2017. The roads ahead: narratives for shared socioeconomic pathways describing world futures in the 21st century. Glob. Environ. Change. 42, 169−180. https://doi.org/10.1016/j.gloenvcha.2015.01.004.

Palmer, W.C., 1965. Meteorological drought. Office of Climatology, Weather Bureau, Washington DC.

Shi, Y., Yongping, S., Ruji, H., 2002. Preliminary study on signal, impact and foreground of climatic shift from warm-dry to warm-humid in Northwest China. J. Glaciol. Geocryol. 24 (3), 219−226. https://doi.org/10.3969/j.issn.1000-0240.2002.03.001 (in Chinese).

Sternberg, T., 2018. Moderating climate hazard risk through cooperation in Asian drylands. Land. 7 (1), 22. https://doi.org/10.3390/land7010022.

Su, B., Huang, J., Fischer, T., et al., 2018. Drought losses in China might double between the 1.5°C and 2.0°C warming. Proc. Natl. Acad. Sci. U. S. A. 115 (42), 10600−10605. https://doi.org/10.1073/pnas.1802129115.

Svoboda, M., Hayes, M., Wood, D., 2012. Standardized precipitation index user guide. World Meteorological Organization, Geneva, Switzerland.

van Loon, A.F., Stahl, K., Di Baldassarre, G., et al., 2016. Drought in a human-modified world: reframing drought definitions, understanding, and analysis approaches. Hydrol. Earth Syst. Sci. 20, 3631−3650. https://doi.org/10.5194/hess-20-3631-2016.

Vicente-Serrano, S.M., Beguería, S., Lopez-Moreno, J.I., 2010. A multiscalar drought index sensitive to global warming: the standardized precipitation evapotranspiration index. J. Clim. 23, 1696−1718. https://doi.org/10.1175/2009JCLI2909.1.

Wang, L., Chen, W., 2014. A CMIP5 multimodel projection of future temperature, precipitation, and climatological drought in China. Int. J. Climatol. 34, 2059−2078. https://doi.org/10.1002/joc.3822.

Wang, X., Dong, Z., Zhang, J., et al., 2004. Modern dust storms in China: an overview. J. Arid Environ. 58, 559−574.

Wang, Y., Qin, D., 2017. Influence of climate change and human activity on water resources in arid region of Northwest China: an overview. Clim. Change Res. 8 (4), 268−278. https://doi.org/10.1016/j.accre.2017.08.004 (in Chinese).

Yang, X., Wood, E.F., Sheffield, J., et al., 2018a. Bias correction of historical and future simulations of precipitation and temperature for China from CMIP5 models. J. Hydrometeorol. 19 (3), 609−623. https://doi.org/10.1175/JHM-D-17-0180.1.

Yang, P., Xia, J., Zhan, C., et al., 2018b. Discrete wavelet transform-based investigation into the variability of standardized precipitation index in Northwest China during 1960−2014. Theor. Appl. Climatol. 132 (1−2), 167−180. https://doi.org/10.1007/s00704-017-2063-3.

Yao, N., Li, L., Feng, P., et al., 2020. Projections of drought characteristics in China based on a standardized precipitation and evapotranspiration index and multiple GCMs. Sci. Total Environ. 704, 135245. https://doi.org/10.1016/j.scitotenv.2019.135245.

Yuan, Q., Wu, S., Dai, E., et al., 2017. Spatio-temporal variation of the wet-dry conditions from 1961 to 2015 in China. Earth Sci. 60 (11), 2041−2050. https://doi.org/10.1007/s11430-017-9097-1.

Zhang, F., Lei, Y., Yu, Q., et al., 2017. Causality of the drought in the southwestern United States based on observations. J. Clim. 30 (13), 4891−4896. https://doi.org/10.1175/JCLI-D-16-0601.1.

Zhang, L., Chen, X., Xin, X., 2019a. Short commentary on CMIP6 Scenario Model Intercomparison Project (ScenarioMIP). Clim. Change Res. 15 (5), 519−525. https://doi.org/10.12006/j.issn.1673-1719.2019.082 (in Chinese).

Zhang, Q., Fan, K., Singh, V.P., et al., 2019b. Is Himalayan-Tibetan Plateau "drying"? Historical estimations and future trends of surface soil moisture. Sci. Total Environ. 658, 374−384. https://doi.org/10.1016/j.scitotenv.2018.12.209.

Zhang, Y., He, B., Guo, L., et al., 2019c. The relative contributions of precipitation, evapotranspiration, and runoff to terrestrial water storage changes across 168 river basins. J. Hydrol. 579, 124194. https://doi.org/10.1016/j.jhydrol.2019.124194.

Zhou, W., Gang, C., Zhou, F., et al., 2015. Quantitative assessment of the individual contribution of climate and human factors to desertification in northwest China using net primary productivity as an indicator. Ecol. Indic. 48, 560−569. https://doi.org/10.1016/j.ecolind.2014.08.043.

Zhu, H., Jiang, Z., Li, J., et al., 2020. Does CMIP6 inspire more confidence in simulating climate extremes over China? Adv. Atmos. Sci. 37, 1119−1132. https://doi.org/10.1007/s00376-020-9289-1.